Anti-Cancer Drugs 2002, **13,** pp. 1017–1029

Preclinical report

Colocalization of BAX with BID and VDAC-1 in nimesulide-induced apoptosis of human colon adenocarcinoma COLO 205 cells

Michat Marek Godlewski,[1] Barbara Gajkowska,[2] Monika Lamparska-Przybysz[1] and Tomasz Motyl[1]

[1]Department of Physiological Sciences, Faculty of Veterinary Medicine, Warsaw Agricultural University, 02-776 Warsaw, Poland. [2]Laboratory of Cell Ultrastructure, Medical Research Centre, Polish Academy of Science, 02-106 Warsaw, Poland.

Cyclooxygenase (COX)-2 inhibitors that belong to non-steroid anti-inflammatory drug family have been shown to have an apoptosis-inducing effect on neoplastic cells. In the present study the effect of nimesulide (NIM), a specific COX-2 inhibitor, on apoptosis and interactions between BCL-2 family death promoters BAX and BID and BAX and VDAC-1 were examined in human colon adenocarcinoma COLO 205 cells. Laser scanning cytometry was applied for the measurement of expression and aggregation of apoptosis-related proteins and quantitative analysis of NIM-induced apoptosis. Double-staining immunoconfocal and immunoelectron microscopy were used for subcellular colocalization of examined proteins. NIM induced apoptosis of COLO 205 cells in a dose-dependent manner. This was accompanied by: (1) a decrease in intracellular prostaglandin (PG) E_2 content; (2) subcellular redistribution and aggregation of BAX and BID on organellar membranes and within the nucleus; (3) colocalization of BAX with BID and BAX with VDAC-1 on organelles; and (4) survival of cells with the highest BCL-2 aggregation. A similar pattern of subcellular redistribution and colocalization of BAX with BID and BAX with VDAC-1 suggests that BAX (in association with BID) controls the function of VDAC-1 and its permeability for apoptogenic factors released from mitochondria of COLO 205 cells stimulated to apoptosis with NIM. [© 2002 Lippincott Williams & Wilkins.]

Key words: Apoptosis, BAX, BID, COLO 205, nimesulide, prostaglandin E_2, VDAC-1.

Introduction

BAX, a 21-kDa protein, is regarded as a tumor suppressor which sensitizes malignant cells to anticancer drugs.[1–4] Our recent study indicated that in spite of different molecular mechanisms of apoptosis induced by various anticancer drugs, BAX remains the common link in the chain of reactions leading to the cell death.[5] On the other hand, mutations in the *bax* gene protect tumor cells against apoptogenic effects of anticancer drugs.[6,7] In spite of intensive studies, the molecular mechanism of the proapoptotic action of BAX remains unclear. It is suggested that BAX oligomerizes and forms ion channels or, together with other proteins (VDAC-1, ANT and cyclophilin D), forms permeability transition pore complexes in the outer mitochondrial membrane, which in turn facilitates the release of cytochrome *c*, procaspase-9 and AIF from the mitochondrial intermembrane space.[8–10] Cytochrome *c* and procaspase-9 form a complex with cytosolic Apaf-1 that eventually leads to the activation of the caspase cascade and caspase-dependent DNase. AIF degrades nuclear proteins and partly DNA (to about 50-kb fragments) independently of caspases and DNases.[11] The movement of BAX from the cytosol to the mitochondria during apoptosis is completed within 30 min, and precedes cell shrinkage and chromatin condensation.[12] Our previous experiments[5,13] and those performed by Mandal *et al.*[14] showed that apart from moving to mitochondria, BAX is translocated to the Golgi apparatus, endoplasmic reticulum and via nuclear envelope pores to the nucleus in cells stimulated to apoptosis. Moreover, we found an increase in BAX immunoreactivity on fine filaments and the lamina-pore complexes of the nuclear matrix of camptothecin-treated COLO 205 cells.[15] It is believed that BAX translocation from cytosol to organellar membranes is dependent on its activation by *m*-calpain,[16] BID[17]

Correspondence to T Motyl, Department of Physiological Sciences, Faculty of Veterinary Medicine, Warsaw Agricultural University, Nowoursynowska 159, 02-776 Warsaw, Poland.
Tel/Fax: (+48 22) 847 24 52;
E-mail: t.motyl@hotmail.com.

or Bif-1.[18] The BH3 domain is exposed during BAX activation, which permits BAX oligomerization.[19–21] Oligomerization of BAX relies on conformational changes resulting in hydrophobic domain exposure and anchoring in membrane lipids.[20] The results of our previous study indicate that activation of BAX, occurring through proteolytic cleavage of the N-terminal epitope and BH3 motif exposure, is the condition for BAX translocation to organelles in COLO 205 cells under the influence of anticancer drugs.[5] It is interesting that BID (being the BH3-only protein) facilitates BAX translocation from the cytosol to organellar membranes in the tumor cells exposed to staurosporine.[22] BID's activity is regulated by a caspase-8-mediated cleavage event, exposing the BH3 domain, and significantly changing the surface charge and hydrophobicity, resulting in a change in cellular localization.[23] It is suggested that BID binds to BAX and allows the conformation of BAX, leading to its oligomerization and insertion into the outer mitochondrial membrane.[17]

In the present study we used laser scanning cytometry (LSC) and double-staining confocal and immunoelectron microscopy to examine BAX, BID and VDAC-1 redistribution and colocalization in human colon adenocarcinoma COLO 205 cells induced to apoptosis by nimesulide (NIM). NIM, a non-steroid anti-inflammatory drug, is a specific cyclooxygenase (COX)-2 inhibitor,[24] and possesses antineoplastic and proapoptotic properties.[5,25–28] Results of this study reveal the involvement of BCL-2-related death promoters (BAX and BID) in NIM-induced apoptosis in COLO 205 cells. Moreover, we observed a colocalization of BAX with BID and BAX with VDAC-1 on organellar membranes of cells stimulated to apoptosis.

Materials and methods

Media and reagents

DMEM powdered medium (without L-glutamine), L-glutamine, phosphate-buffered saline, pH 7.4. (PBS), FCS, fungizone and gentamycin sulfate were obtained from Gibco/BRL (Paisley, UK). Polyclonal rabbit anti-human BAX, polyclonal mouse anti-human BCL-2 FITC-conjugated antibodies and non-specific rabbit immunoglobulin fraction were supplied by Dako (Glostrup, Denmark); monoclonal goat anti-BID and anti-VDAC antibodies were supplied by Santa Cruz Biotechnology (Santa Cruz, CA). Anti-human PGE_2 whole rabbit antiserum was from Sigma-Aldrich (Schnelldorf, Germany). FITC-conjugated $F(ab')_2$ fragment of swine anti-rabbit immunoglobulin was from Dako and Alexa Fluor 546 donkey anti-goat secondary antibody was purchased from Molecular Probes (Eugene, OR). Colloidal gold 30 nm donkey anti-rabbit and 20 nm donkey anti-goat conjugated immunoglobulins were from Jackson ImmunoResearch (West Grove, PA). Horseradish peroxidase (HRP)-conjugated goat anti-rabbit IgG (H + L) was supplied by Bio-Rad (Hercules, CA). ECL Western blotting detection reagents and Hyperfilm ECL were purchased from Amersham Pharmacia Biotech (Little Chalfont, UK). NIM, aspirin (ASP) and other chemicals were from Sigma (St Louis, MO). Sterile conical flasks, eight-chamber culture slides and sterile disposable pipettes were purchased from Nunc (Naperville, IL).

Cell culture

Human tumor cell line, colon adenocarcinoma COLO 205, was obtained from the ATCC (Rockville, MD). Cell cultures were maintained in DMEM supplemented with 10% (v/v) FCS, 0.2% (w/v) L-glutamine, 50 μg/ml gentamycin and 2.5 μg/ml fungizone (10%FCS/DMEM) in an atmosphere of 5% CO_2/95% humidified air at 37° C, and routinely subcultured every 2 or 3 days.

Drugs

Drugs were diluted in DMSO to create stock solutions which were stored according to the manufacturer's suggestions. Final solutions used in experiments were: 1 and 50 μM NIM and 125 μM ASP.

Experimental procedure and immunofluorescence staining

Exponentially growing cells were transformed to the eight-chamber culture slides, cultured for 24 h and then incubated with the drugs in 10% FCS/DMEM for up to 6 h. The control cultures were treated with equivalent concentrations of DMSO suspended in 10% FCS/DMEM. Then cells were fixed in 0.25% formaldehyde for 15 min, washed twice with PBS, suspended in ice-cold 70% methanol and stored at 2°C for 30 min. Afterwards methanol was aspirated and samples were stored in –80°C until staining. The cells were washed twice with PBS/1% BSA and incubated for 1 h with either primary antibody

diluted 1:250 with PBS/1% BSA. After primary incubation, the cells were washed twice with PBS/1% BSA and incubated for 1 h with 1:250 (Dako) or 1:500 (Molecular Probes) secondary antibodies. The cells were then washed twice in PBS/1% BSA and finally incubated with 5 μg/ml solution of 7-aminoactinomycin D (7-AAD) for 30 min to counterstain the DNA. Then the chamber walls were removed and coverslips were mounted on microscope slides using an anti-fade mounting medium (ICN, Aurora, OH).

PGE_2 detection

Rabbit anti-human PGE_2 antiserum (Sigma-Aldrich Chemie) was diluted and stored according to the manufacturer's suggestions. Cell cultures were prepared and stained as described above, with exception of no BSA supplement. As a negative control, cells labeled with the non-specific rabbit immunoglobulin fraction (Dako) and the FITC-conjugated anti-rabbit secondary antibody (Dako) were used. PGE_2-related fluorescence in COLO 205 cells was analyzed by LSC.

LSC

Probes were analyzed by LSC (CompuCyte, Boston, MA). At least 3×10^3 cells per chamber area were analyzed. The fluorescence excitation was provided by a 488 nm, 10 mW Argon laser beam. The green fluorescence of FITC-labeled antibody was measured using a combination of dichroic mirrors and filters transmitting at 520 $\pm$ 20 nm wavelength (detector offset and gain set to 2000 and 32, respectively), and far-red fluorescence of 7-AAD transmitting at above 650 nm (offset 2000 and gain 30). BAX-associated green fluorescence was measured separately over the nucleus (Nf) and the cytoplasm (Cf). Nf was measured within the area outlined by the 'integration contour', located 1 pixel outside the 'threshold contour' triggered by the far-red fluorescence of 7-AAD. Cf was measured within the rim of cytoplasm 9 pixels wide, located outside the 'integration contour'. The background green fluorescence was automatically measured within 2 pixels range outside the 'peripheral contour', and subtracted from both nuclear and cytoplasmic green fluorescence, to obtain the final values of Nf and Cf, respectively. Another parameter measured was BAX maximal pixel (BAX MP) corresponding to the highest value of BAX-related fluorescence in the cell, regardless of cellular compartment. Obtained results were analyzed by Excel 2000 software (Microsoft, Redmond, WA).

Confocal microscopy

Cells were double stained with FITC-conjugated anti-BAX antibodies, and, separately, with Alexa Fluor 546-conjugated anti-BID and anti-VDAC. Then cells were visualized by confocal LSC using the FV-500 system (Olympus, Hamburg, Germany). The combinations of excitation/emission were: argon 488 nm laser versus 505–525 nm filter for FITC and HeNe 543 nm laser versus 610 nm filter for Alexa Fluor 546. Stacks of cross-sections from representative control and early apoptotic cells (1 h incubation with NIM) were gathered separately for each fluorescence channel. Three-dimensional images and series of cross-sections were reconstructed using the Fluoview program (Olympus).

Postembedding immunogold labeling

Ultrathin sections of Epon-embedded specimens were prepared using diamond knives. The sections were picked up on nickel grids covered with formvar, incubated in 10% hydrogen peroxide for 10 min and rinsed in PBS for 15 min.For double labeling of Bax (dilution 1:20) with Bid (dilution 1:50) and Bax with VADC-1 (dilution 1:100) sections were incubated with rabbit anti-Bax primary antibody for 2 h and then with goat anti-Bid for 4 h, and with anti-Bax primary antibody or 2 h and anti-VADC-1 for 4 h. The secondary antibodies were applied as mixtures of both secondary goat anti-rabbit (dilution 1:50; BBInternational, Cardiff, UK, batch 3407) and rabbit anti-goat (dilution 1:20; BBInternational; batch 3326) immunoglobulins decorated with 30 and 20 nm gold particles, respectively. The incubation period was 1–2 h at the secondary antibody step in double-labeling protocols. All immunolabeling steps were carried out at 37°C. After immunolabeling, the sections were washed with PBS and distilled water, dried, and stained with uranyl acetate and lead citrate. All sections were examined in Joel 1200EX electron microscope. In negative controls primary antibodies were omitted or the sections were incubated with irrelevant primary antibody. These controls demonstrated no labeling.

Western blot analysis

Proteins were isolated according to method described previously (5). Then samples containing identical quantities of proteins were subjected to

SDS–PAGE (12.5% gel) together with Kaleidoscope and Low Range Marker. The electrophoresis was performed for 1.5 h at 100 V using a Mini Protean II apparatus (Bio-Rad). After electrophoresis, separated proteins were electroblotted on a Sequi-Blot PVDF Membrane for Protein Sequencing for 1 h at 100 V using a Mini Protean II* apparatus. The membranes were blocked with 5% solution of non-fat dry milk in TBST (pH 7.5) for 16 h at 4°C, washed 3 times for 10 min in TBST at room temperature, and incubated with diluted 1:200 rabbit anti-human BAX and goat anti-human BID monoclonal antibodies at 37°C for 2 h. The membranes were then washed as described above and incubated with a mixture of diluted 1:500 donkey anti-rabbit and donkey anti-goat IgG antibodies conjugated with HRP at 37°C for 2 h. Afterwards the membranes were washed as above, and visualized using the ECL Western blotting detection reagents and Hyperfilm ECL high performance chemiluminescence film. Developed films were scanned and analyzed using Electrophoresis Documentation and Analysis System EDAS 290 with 1D Image Analysis Software (Eastman Kodak, Rochester, NY).

Statistical evaluation

The results were statistically evaluated by ANOVA and Tukey's multiple-range tests using Microcal Origin 6.0. (Microcal, Northampton, MA). $p \leqslant 0.05$ was regarded as significant and $p \leqslant 0.01$ as highly significant.

Results

NIM induces apoptosis in COLO 205 cells

LSC scans of COLO 205 cells treated with increasing concentrations of NIM (the COX-2 inhibitor) revealed an increase in apoptotic cell number (measured by the percentage of cells in sub-G_1 peak) apparent at 1 μM concentration (Figure 1a). Interestingly there seemed to be a 'plateau' in cell response to NIM concentrations between 1 and 25 μM (10.7, 11.2 and 11.8%, respectively). The second increase in apoptotic cell number occurred at a NIM concentration of 50 μM. The gallery of cells on Figure 1(b) represents relocated cells from measured areas, showing typical features of apoptosis, i.e. cell shrinkage, chromatin condensation and margination, nuclear pyknosis, and formation of apoptotic bodies. For further experiments we used 1 and 50 μM NIM concentrations that proved to significantly increase apoptosis in COLO 205 cells. Parallel experiments conducted with 125 μM ASP (the COX-1 inhibitor) revealed no significant changes in the number of apoptotic cells (Figure 1a).

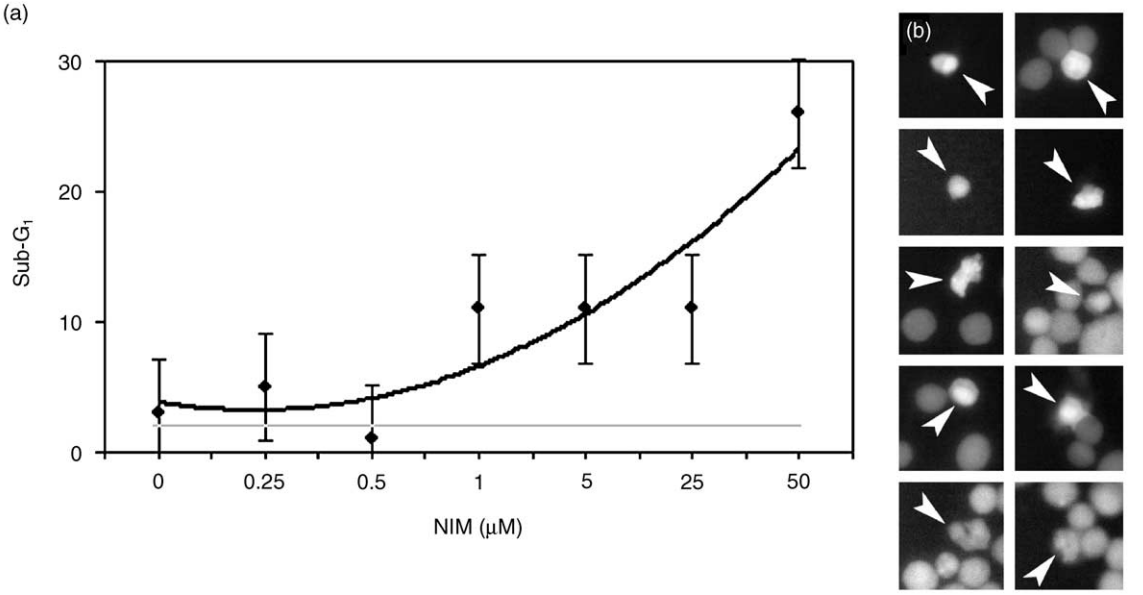

Figure 1. Percent of apoptotic cells ± SEM in COLO 205 control culture (0 μM NIM) and in cultures treated with increasing concentrations of NIM (a). (b) Gallery of cells with typical features of apoptosis, i.e. DNA condensation and margination, nucleus fragmentation, and formation of apoptotic bodies (cells marked with arrows). Apoptotic cells were relocated using CompuSort.

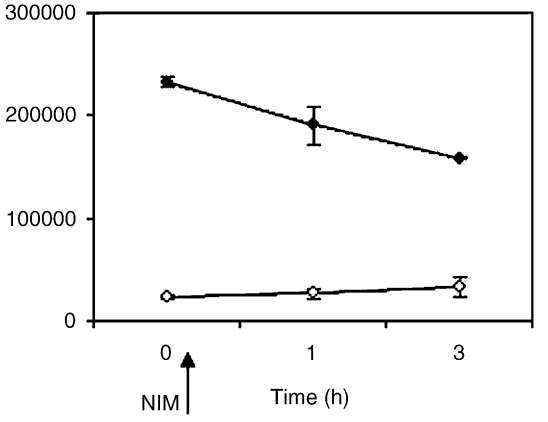

Figure 2. Changes in PGE_2-related fluorescence in COLO 205 cells treated with 1 μM NIM for 1 and 3 h measured by LSC (full dots). As a negative control, the fluorescence related to non-specific rabbit immunoglobulin fraction was measured (empty dots). Results are presented as means $\pm$ SEM from three different experiments; at least 15×10^3 cells per sample were analyzed.

Furthermore 1 μM NIM treatment significantly decreased PGE_2-related fluorescence in COLO 205 cells, the while no changes were observed in negative control cultures labeled with non-specific rabbit immunoglobulin fraction (Figure 2).

Survival of COLO 205 cells is dependent on BCL-2 expression

Since Bcl-2 plays a distinct role in cell survival, its expression was analyzed in cultures of COLO 205 cells incubated with 50 μM of NIM for 6 h, followed by 24 h incubation in the growth-promoting medium (10% FCS/DMEM). The expression of the Bcl-2 was considerably higher in the surviving population of cells than in control cells (CTRL) non-exposed to NIM (Figure 3c). Moreover, the aggregation of Bcl-2 protein in NIM-treated cells increased from 4.4 to 92.6% (Figure 3, *cf* a and b).

Subcellular redistribution of BAX and BID

After 1 h incubation with 1 μM NIM a significant increase in BAX MP from 9 to 49% was observed (Figure 4a and b). BAX MP slowly decreased during next 2 h to the level of 20% (Figure 4c). Changes in BID MP occurred simultaneously to those of BAX (from 28% before to 95 and 94% after 1 and 3 h, respectively; Figure 4d–f). Generally BID was more aggregated than BAX during NIM-induced apoptosis and even in non-treated cultures (Figure 4, *cf* upper and lower panels).

During the first hour of cell exposure to NIM there was a significant change in BAX and BID subcellular localization. LSC analysis showed that expression of both proteins in the nuclear area of the cell increased dramatically (Figure 5a and c), which was accompanied by less pronounced changes in the cytoplasmic area (Figure 5b and d). A similar pattern of changes was observed by Western blotting (Figure 6). There was a significant increase in BAX and BID IOD both in nuclear and cytoplasmic fraction 1 h after NIM treatment that corresponded with the results acquired with the use of LSC.

BAX–BID colocalization

Colocalization of BAX and BID was visualized using immunoconfocal and immunoelectron microscopy. Confocal images revealed separate BAX-related

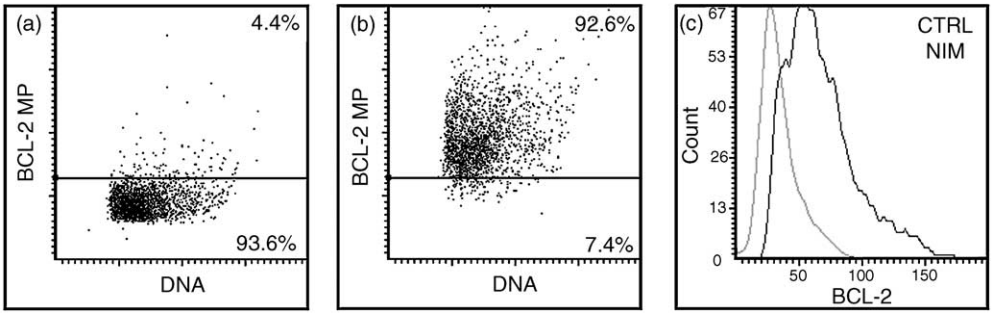

Figure 3. Cytograms showing changes in percentage of COLO 205 cells with high BCL-2-MP in control culture (a) and after 6 h of NIM treatment (50 μM) followed by 24 h incubation in growth medium (10% FCS/DMEM) (b). Increase in BCL-2 expression can be also observed when comparing histogram of the control culture (CTRL, gray line) with one treated as described with NIM (NIM, black line) (c).

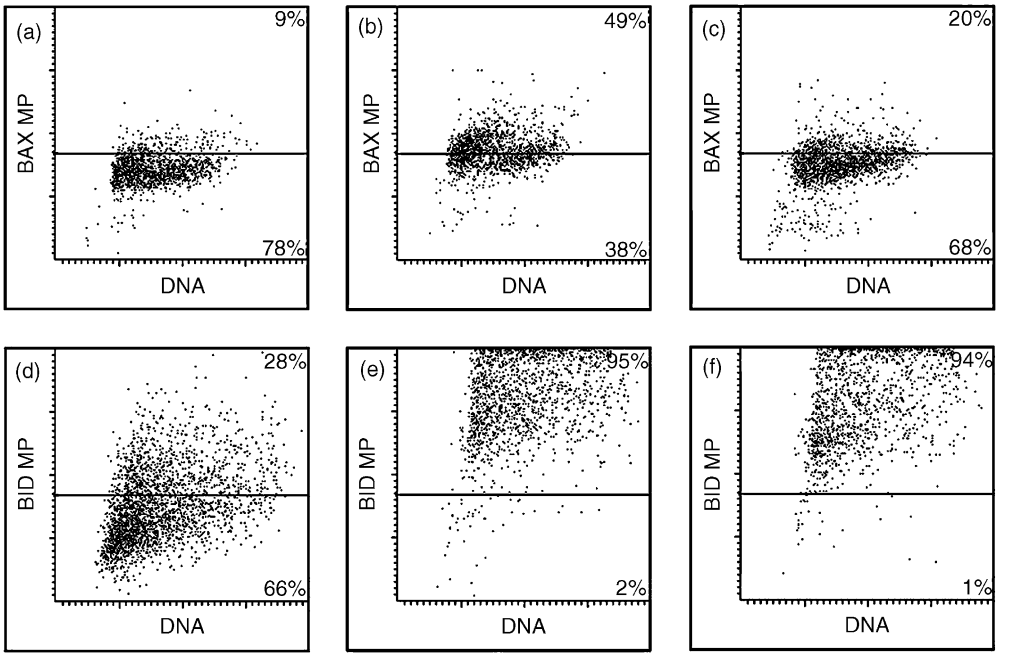

Figure 4. Changes in percentage of COLO 205 cells showing high BAX-MP (upper panel) and high BID-MP (lower panel) in control cultures (a and d), and after 1 (b and e) and 3 h (c and f) of cell exposure to NIM. Cytograms are representative of three experiments.

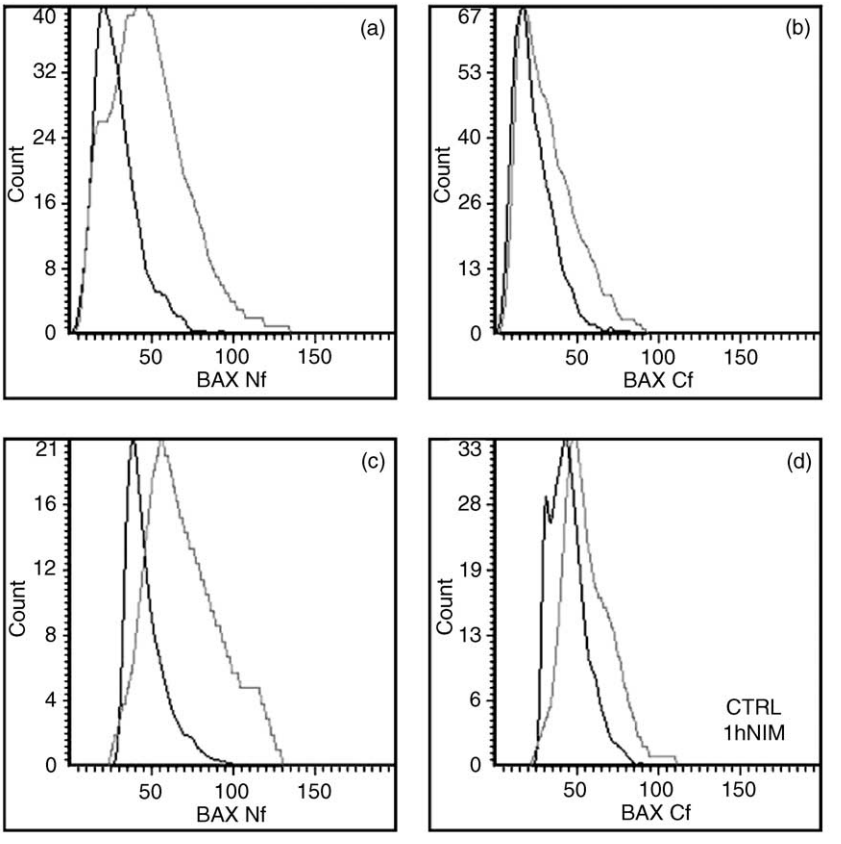

Figure 5. Increase in BAX Nf (a) and Cf (b), and BID Nf (c) and Cf (d) occurs after 1 h of COLO 205 cell exposure to NIM (1 μM). Control cultures are represented by black lines (CTRL) and NIM-treated cultures gray lines (1 h NIM). Histograms are representative of three experiments.

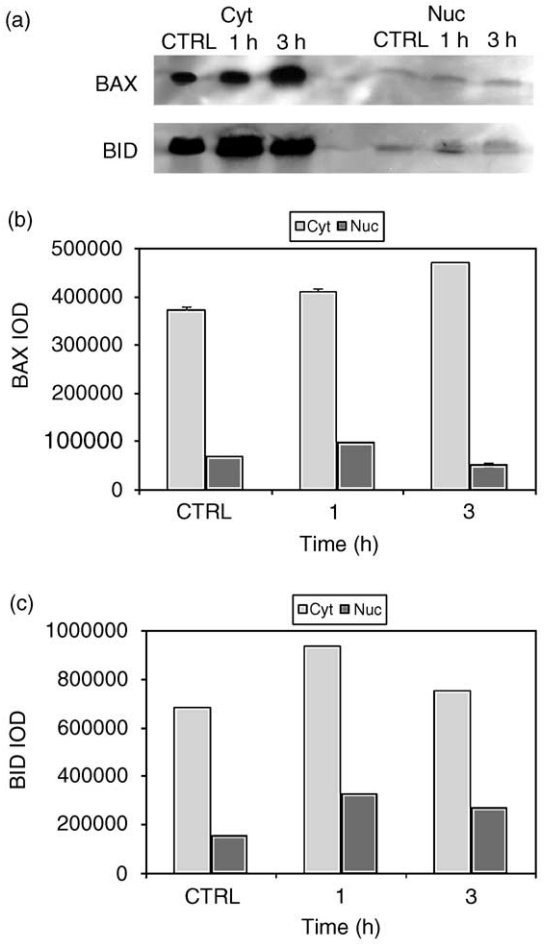

Figure 6. Western blot analysis of BAX and BID in COLO 205 cells stimulated to apoptosis by NIM (1 μM). After NIM treatment there was an increase in area and intensity of bands (a, *cf* CTRL with 1 and 3 h). BAX (b) and BID (c) IOD ($\pm$SEM) was evaluated using 1D Image Analysis Software. Data for IOD analysis was acquired from three different experiments.

fluorescence (green) and BID-related fluorescence (red) in control cells, cultured in growth-promoting medium (10% FCS/DMEM) (Figure 7a). The sequence of cross-sections showed a uniform distribution of BAX within the cell and cytoplasmic localization of BID. The cells stimulated to apoptosis with NIM (1 μM) showed a strong pattern of colocalization between two fluorescence marked proteins, appearing as a strong yellow light generated by simultaneous excitation of both fluorescent dyes (Figure 7b). Colocalization of BAX and BID was visible both in the cytoplasm and nucleus.

A more spectacular colocalization of both death promoters was shown on immunoelectron microphotographs, where BAX and BID are represented by different diameter gold particles (Figure 8). The clusters consisting of BAX and BID-related gold particles were localized on mitochondria (Figure 8a, e and f), rough endoplasmic reticulum (not shown), nuclear envelope pore (Figure 7d) and within the nucleus (Figure 8b and c) of COLO 205 cells stimulated to apoptosis with NIM (1 μM).

BAX–VDAC-1 colocalization

In control cells there was no detectable colocalization of BAX and VDAC-1. Green BAX-related fluorescence was localized in both cell compartments (cytoplasmic and nuclear), whereas red VDAC-1-related fluorescence was present only in the cytoplasmic area (Figure 9a). After induction of apoptosis, subsequent cross-sections showed a strong pattern of colocalization between BAX and VDAC-1 (yellow light) within the cytoplasm and the nucleus (Figure 9b). The strong green, BAX-related fluorescence emitted from aggregated BAX particles was noted. To visualize the subcellular colocalization of BAX and VDAC-1 in NIM-treated cells, immunogold double-staining was performed (Figure 10). BAX and VDAC-1 colocalization on mitochondria (Figure 10Ac, B and C), rough endoplasmic reticulum (Figure 10Ab), nuclear envelope pore (Figure 10Aa) and within the nucleus (Figure 10Ab) was observed.

Discussion

The presented results revealed a dose-dependent apoptotic effect of NIM in human colon adenocarcinoma COLO 205 cells (Figure 1), which is compatible with its suppressive effect on experimental colon carcinogenesis.[25,29] Since NIM is a selective inhibitor of COX-2,[30] its apoptogenic influence is probably associated with impaired activity of this enzyme. This was proved by analysis conducted with the use of anti-PGE_2 antiserum, which showed a significant decrease in intracellular PGE_2 levels after NIM treatment (Figure 2). Selective inhibitors of COX-2 have been demonstrated to induce apoptosis in a variety of cancer cells, including those of the colon, stomach, breast and prostate.[31] Moreover, the increase in tumorigenic potential by COX-2 overexpression is associated with resistance of tumor cells to apoptosis.[32–35] In contrast, the inhibition of COX-1 by ASP did not induce apoptosis in COLO 205 cells (Figure 1a), which may suggest that triggering of apoptosis is dependent on COX-2, rather then on

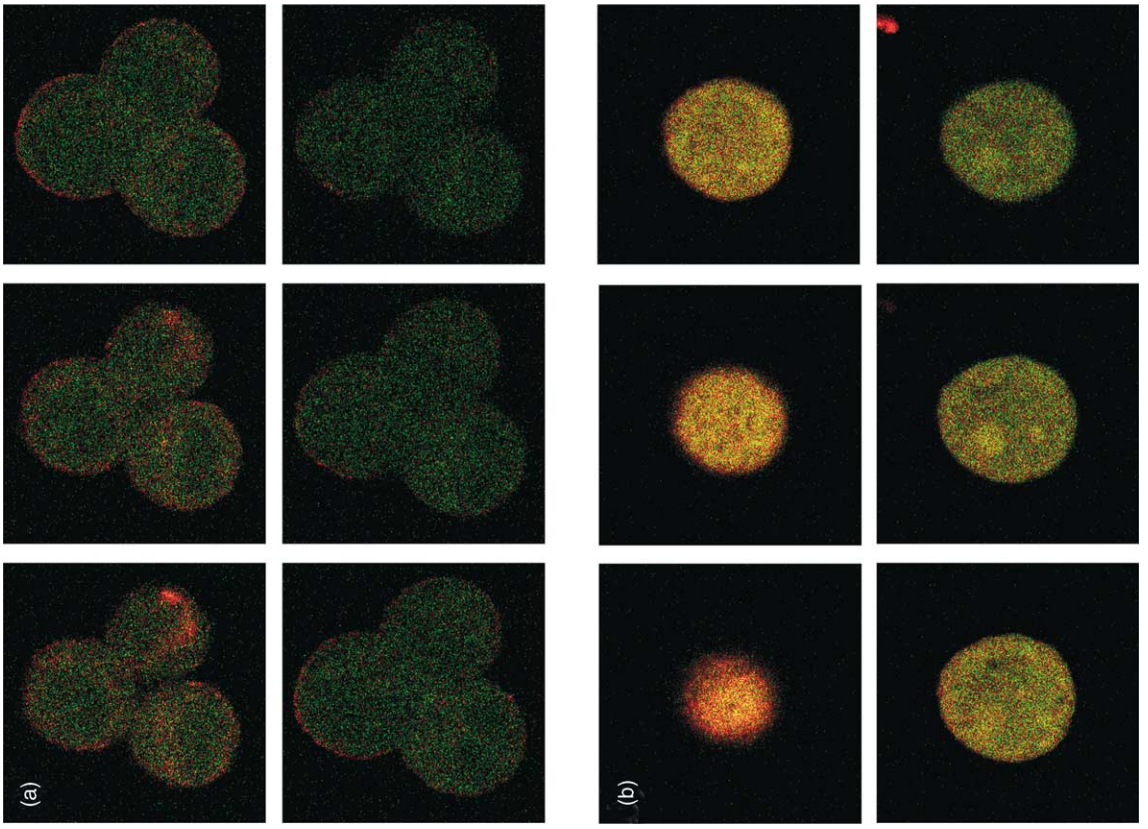

Figure 7.

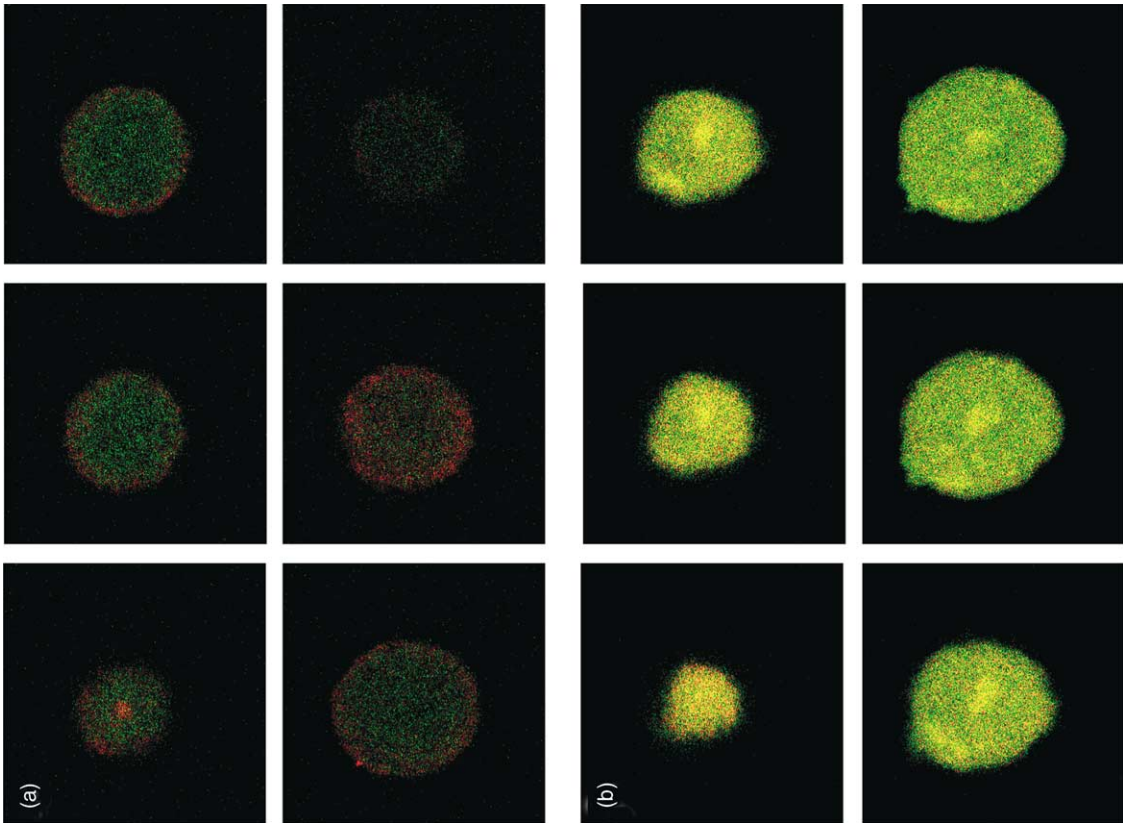

Figure 9.

COX-1 activity. Similar effects were obtained with another COX-2 inhibitor (celecoxib) in HTC-IR cells (data not shown). Since ASP is able to induce apoptosis in HeLa cells,[36] it is possible that the effect of ASP is dependent on cell type.

The biochemical mechanism of apoptosis induction by NIM and other NSAIDs is still obscure. There are several hypotheses, including activation of the ceramide pathway,[37] blocking the activation of the anti-apoptotic kinase Akt (protein kinase B),[31] down-regulation of the anti-apoptotic protein BCL-2,[38,39] and up-regulation of NAG-1[40] and prostate apoptosis response 4 (*par-4*) gene.[27] In our study we focused attention on the role of BCL-2-related proteins in the regulation of NIM-induced apoptosis. It has been clearly shown that survival of NIM-treated COLO 205 cells is dependent on BCL-2 expression. After 6 h of cell culture exposure to NIM (50 μM), a reduction in cell number accompanied by an increase in BCL-2 expression was observed (Figure 3). It is probably due to the natural selection of cells and survival of those with the highest BCL-2 content. Another possibility is that the increase in BCL-2 synthesis is the result of adaptation to prolonged exposure to the apoptogenic factor. A similar phenomenon was observed in other neoplastic cells induced to apoptosis by oxidative stress[41] and starvation.[42]

The results presented here show that NIM-induced apoptosis in COLO 205 cells is dependent on subcellular redistribution and interaction of two death promoters: BAX and BID. Subcellular redistribution of BAX and BID was shown as the increase in BAX-MP and BID-MP within 1 h after NIM administration (where MP is regarded as a marker of molecules aggregation) (Figure 4). BAX- and BID-related fluorescence was elevated both in the nuclear and cytoplasmic area of NIM-treated cells (Figure 5), which was confirmed by increased BAX and BID content measured by Western blotting (Figure 6). More precise localization of BAX and BID was possible using immunoelectron microscopy, showing their aggregates on organellar membranes (mitochondrial, rough endoplasmic reticulum and nuclear envelope) and within the nucleus (Figures 8 and 10). Our previous study demonstrated that BAX redistribution in COLO 205 cells is a common feature of apoptosis induced by various anticancer drugs.[6] BAX and BID subcellular redistribution in response to an apoptotic signal is dependent on their activation that occurs through the proteolytic cleavage at the N-terminus and exposure of the BH-3 domain. This leads to BAX oligomerization, and an interaction of BAX and BID molecules.[5,16,23] It was shown that BAX and BID are cleaved by the action of *m*-calpain and caspase-8, respectively.[11,23,43]

The role of interaction of BAX and BID in the apoptotic process is still controversial. According to one hypothesis, BID as a 'death ligand' devoid of a transmembrane domain can facilitate the insertion of BAX into the mitochondrial membrane to form functional oligomers.[17] This hypothesis is in the line with the fact that BH3 peptide alone, acting like the 'BH3-only' protein BID, mediates cytochrome *c* efflux by oligomerization and insertion of BAX into the mitochondrial membrane.[44] According to another hypothesis, BID possesses the biochemical activity to induce cytochrome *c* release through a mechanism independent of mitochondrial permeability transition pore and BAX.[45] Kudla *et al.*[43] suggest a dual role for BID: (i) a BH3-independent permeabilization of mitochondrial membranes and (ii) a BH3-dependent activation of BAX or inhibition of BCL-X_L. Our study by double-staining confocal and immunoelectron microscopy shows the

Figure 7. Colocalization of BAX and BID analyzed by confocal double staining of COLO 205 cells. In the cell cross-sections from non-treated culture (a) no pattern of colocalization between BAX (green fluorescence) and BID (red fluorescence) was observed. BAX was commonly distributed throughout the cell compartments, whereas BID was localized within the cytoplasm. In the culture treated with 1 μM of NIM, a strong pattern of colocalization between BAX and BID can be observed (bright yellow light coming from simultaneous excitation of colocalized red and green fluorochrome). Furthermore, during NIM-induced apoptosis BID was translocated to the nuclear compartment of the cell.

Figure 9. Colocalization of BAX and VDAC-1 analyzed by confocal double staining of COLO 205 cells. In the cell cross-sections from non-treated culture (a) no pattern of colocalization between BAX (green fluorescence) and VDAC-1 (red fluorescence) was observed. BAX was commonly distributed throughout the cell compartments, whereas VDAC-1 was localized within the cytoplasm. In contrast, in the culture treated with 1 μM of NIM, a strong pattern of colocalization between BAX and VDAC-1 can be observed (bright yellow light coming from simultaneous excitation of colocalized red and green fluorochrome). Furthermore, during NIM-induced apoptosis VDAC-1 was translocated to the nuclear compartment of the cell.

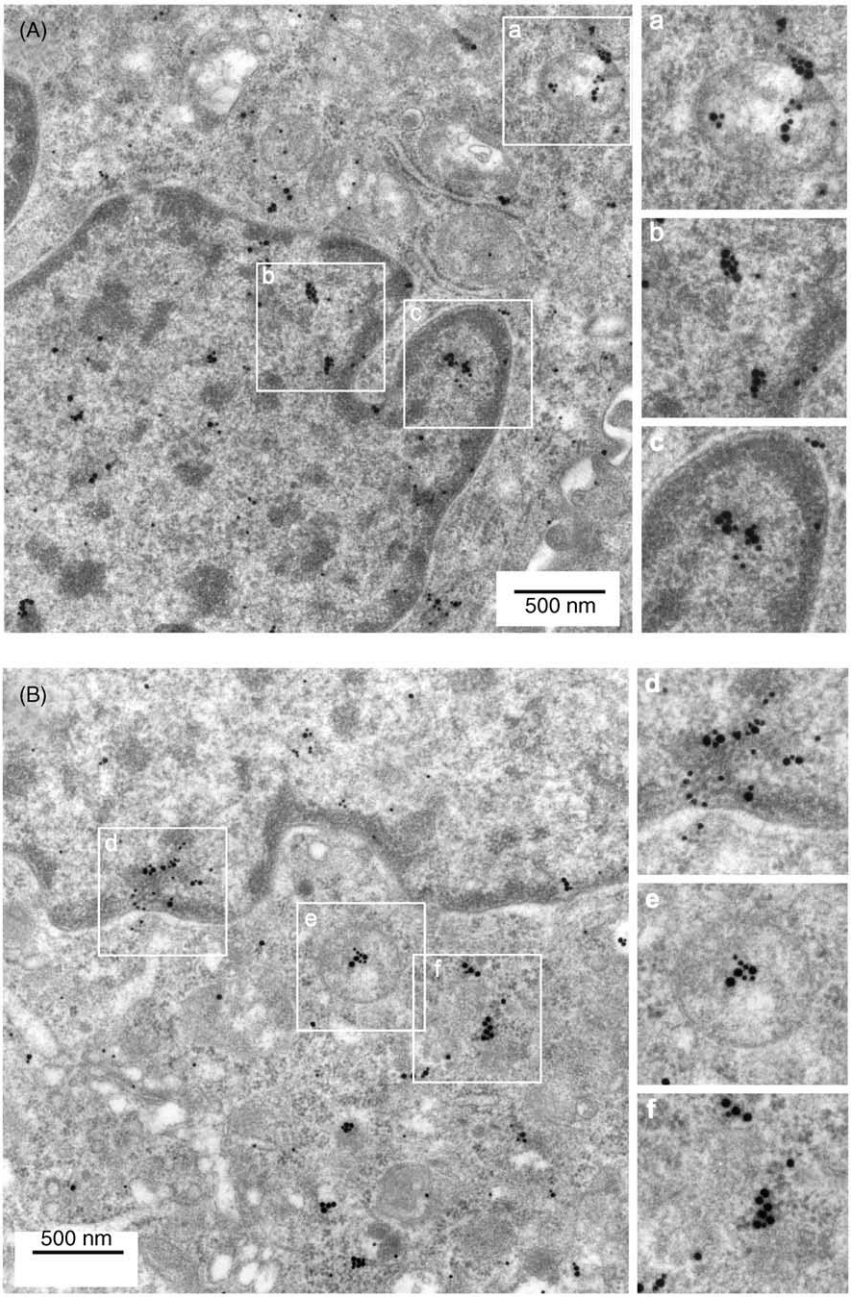

Figure 8. Colocalization of BAX and BID analyzed by immunogold double staining of COLO 205 cells treated with NIM (1 μM) for 1 h (A and B). BAX is represented by 30 nm gold particles and BID by 20 nm gold particles. The clusters consisting of BAX- and BID-related gold particles are localized on mitochondria (a, e and f), nuclear envelope pore (d) and within the nucleus (b and c).

colocalization of BAX and BID in COLO 205 cells induced to apoptosis by NIM (Figures 7 and 8). The presented results may indicate the formation of apoptosis-related heterooligomeric complexes by BAX and BID on organellar membranes (mitochondrial, rough reticulum and perinuclear) and within the nucleus (Figure 8).

Another question is whether BAX-BID complexes form channels in organellar membranes independently or together with other channel-forming proteins (e.g. VDAC-1). Shimizu *et al.*[10] provided evidence that VDAC-1 and BAX create a large pore, with conductance levels 4- and 10-fold greater than those of VDAC-1 and BAX alone. Moreover,

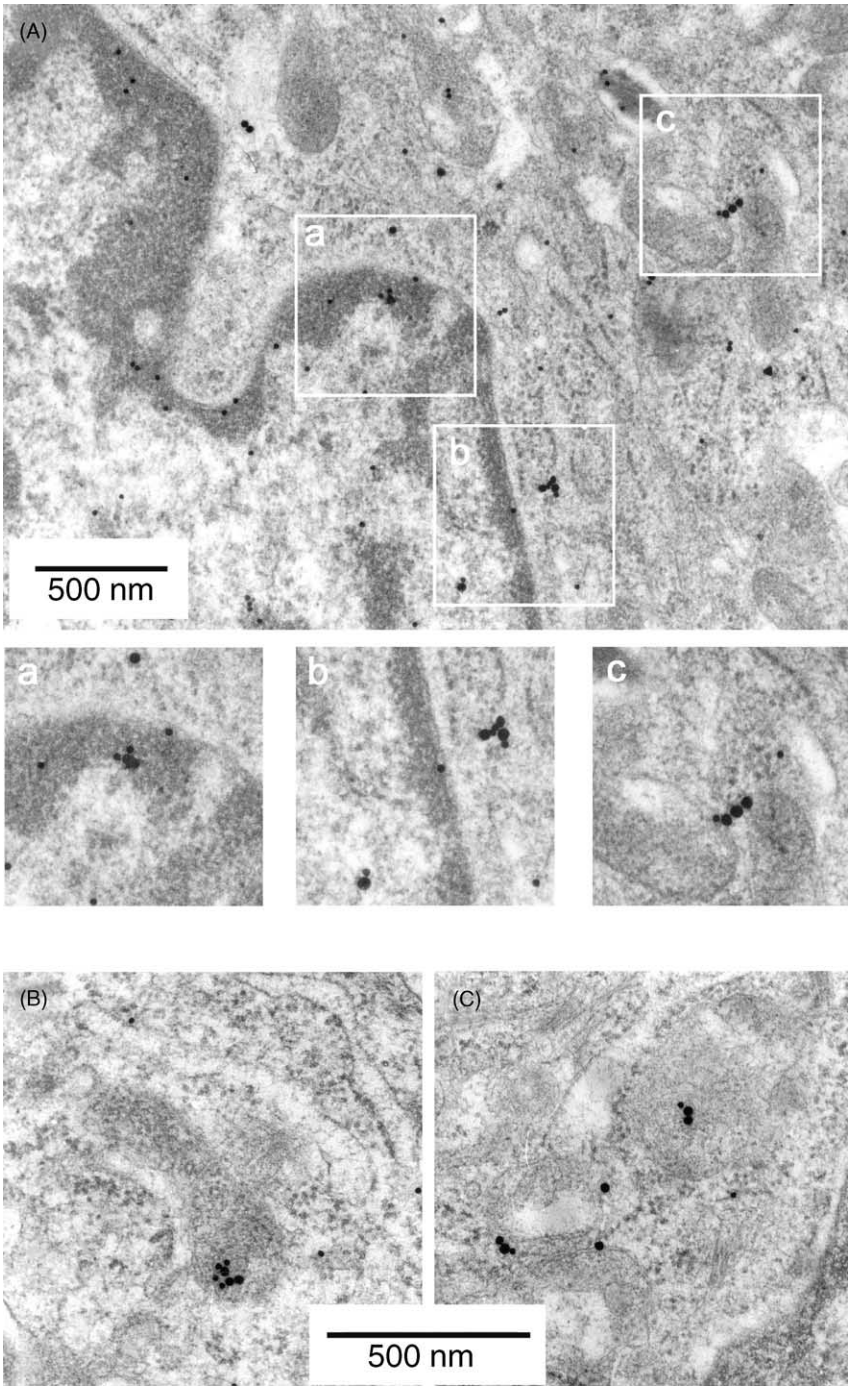

Figure 10. Colocalization of BAX and VDAC-1 analyzed by immunogold double staining of COLO 205 cells treated with NIM (1 μM) for 1 h. BAX is represented by 30 nm gold particles and VDAC-1 by 20 nm gold particles. The clusters consisting of BAX- and VDAC-1-related gold particles are localized on mitochondria (Ac, B and C), rough endoplasmic reticulum (Ab), nuclear envelope pore (Aa) and within the nucleus (Ab).

cytochrome *c* passes through a single VDAC-1–BAX channel but not through the VDAC-1 or BAX channels in a planar lipid bilayer. Our study visualized BAX–VDAC-1 channels by colocalization of these proteins on mitochondrial, rough endoplasmic reticulum and perinuclear membranes of COLO 205 cells stimulated to apoptosis by NIM (Figures 9 and 10). Because most BAX-related gold particles on

organellar membranes associate with VDAC-1 (Figure 10), we suppose that BAX (probably in association with BID) targets VDAC-1 and controls its function. To visualize BID involvement in BAX-VDAC-1 channels, triple-staining immunoelectron microscopy will be used in the subsequent study.

In conclusion, the presented results demonstrate the interaction of BAX and BID in NIM-induced apoptosis of COLO 205 cells, manifested by a similar pattern of changes in subcellular redistribution and their colocalization on organelles. Colocalization of BAX and VDAC-1 suggests that BAX (probably in association with BID) controls the function of VDAC-1 and its permeability for apoptogenic factors released from the mitochondria (e.g. cytochrome *c*, AIF and Smac/DIABLO).

Acknowledgments

This work was supported by grants from the State Committee for Scientific Research 5 P06 K 014 19 and 3 P06 K 035 22.

References

1. Boersma AWM, Nooter K, Burger H, Kortland CJ, Stoter G. Bax upregulation is an early event in cisplatin-induced apoptosis in human testicular germ-cell tumor cell line NT2, as quantitated by flow cytometry. *Cytometry* 1997; **27**: 275–82.
2. Schmitt E, Steyaert A, Cimoli G, Bertrand R. Bax-α promotes apoptosis induced by cancer chemotherapy and accelerates the activation of caspase 3-like cysteine proteases in p53 double mutant B lymphoma namalwa cells. *Cell Death Different* 1998; **5**: 503–16.
3. Kobayashi T, Sawa H, Morikawa J, Zhang W, Shiku H. Bax induction activates apoptotic cascade via mitochondrial cytochrome *c* release and Bax overexpression enhances apoptosis induced by chemotherapeutic agents in DLD-1 colon cancer cells. *Jpn J Cancer Res* 2000; **91**: 1264–8.
4. Nio Y, Iguchi C, Yamasawa K, *et al.* Apoptosis and expression of Bcl-2 and Bax proteins in invasive ductal carcinoma of the pancreas. *Pancreas* 2001; **22**: 230–9.
5. Godlewski MM, Motyl MA, Gajkowska B, Waręski P, Koronkiewicz M, Motyl T. Subcellular redistribution of BAX during apoptosis induced by anticancer drugs. *Anti-Cancer Drugs* 2001; **12**: 607–17.
6. Rampino N, Yamamoto H, Ionov Y, *et al.* Somatic frameshift mutations in the BAX gene in colon cancers of the microsatellite mutator phenotype. *Science* 1997; **275**: 967–9.
7. Yagi OK, Akiyama Y, Nomizu T, Iwama T, Endo M, Yuasa Y. Proapoptotic gene BAX is frequently mutated in hereditary nonpolyposis colorectal cancers but not in adenomas. *Gastroenterology* 1998; **114**: 268–74.
8. Tsujimoto Y, Shimizu S. Bcl-2 family: life-or-death switch. *FEBS Lett* 2000; **466**: 6–10.
9. Tsujimoto Y, Shimizu S. VDAC regulation by the Bcl-2 family of proteins. *Cell Death Different* 2000; **7**: 1174–81.
10. Shimizu S, Ide T, Yanagida T, Tsujimoto Y. Electrophysiological study of novel large pore formed by bax and the voltage-dependent anion channel that is permeable to cytochrome *c*. *J Biol Chem* 2000; **275**: 12321–5.
11. Daugas E, Susin SA, Zamzami N, *et al.* Mitochondria–nuclear translocation of AIF in apoptosis and necrosis. *FASB J* 2000; **14**: 729–39.
12. Wolter KG, Hsu Y-T, Smith CL, Nechushtan A, Xi X-G, Youle RJ. Movement of Bax from the cytosol to mitochondria during apoptosis. *J Cell Biol* 1997; **139**: 1281–92.
13. Motyl T, Gajkowska B, Płoszaj T, Waręski P, Skierski J, Zimowska W. Expression and subcellular redistribution of Bax during TGF-β_1-induced programmed cell death of HC11 mouse mammary epithelial cells. *Cell Mol Biol* 2000; **46**: 175–85.
14. Mandal M, Adam L, Mendelsohn J, Kumar R. Nuclear targeting of Bax during apoptosis in human colorectal cancer cells. *Oncogene* 1998; **17**: 999–1007.
15. Gajkowska B, Motyl T, Olszewska-Bądarczuk H, Godlewski MM. Expression of BAX in cell nucleus after experimentally induced apoptosis revealed by immunogold and embedment free-electron microscopy. *Cell Biol Int* 2001; **25**: 725–33.
16. Gao G, Dou P. N-Terminal cleavage of Bax by calpain generates a potent proapoptotic 18-kDa fragment that promotes Bcl-2-independent cytochrome *c* release and apoptotic cell death. *J Cell Biochem* 2000; **80**: 53–72.
17. Eskes R, Desagher S, Antonsson B, Martinou JC. Bid induces the oligomerization and insertion of Bax into outer mitochondrial membrane. *Mol Cell Biol* 2000; **20**: 929–35.
18. Cuddeback SM, Yamaguchi H, Komatsu K, *et al.* Molecular cloning and characterization of Bif-1: a novel Src homology 3 domain-containing protein that associates with Bax. *J Biol Chem* 2001; **276**: 20559–65.
19. Conus S, Kaufman T, Fellay I, Otter I, Rosse T, Borner C. Bcl-2 is a monomeric protein: prevention of homodimerization by structural constraints. *EMBO J* 2000; **19**: 1534–44.
20. Antonsson B, Montessuit S, Lauper S, Eskes R, Martinou J-C. Bax oligomerization is required for channel-forming activity in liposomes and to trigger cytochrome *c* release form mitochondria. *Biochem J* 2000; **345**: 271–8.
21. Mikhailov V, Mikhailova M, Pulkrabek DJ, Dong Z, Venkatachalam MA, Saikumar P. Bcl-2 prevents Bax oligomerization in the mitochondrial outer membrane. *J Biol Chem* 2001; **276**: 18361–74.
22. Desagher S, Osen-Sand A, Nichols A, *et al.* Bid-induced conformational change of Bax is responsible for mitochondrial cytochrome *c* release during apoptosis. *J Biol Chem* 1999; **144**: 891–901.

23. McDonnell JM, Fushman D, Milliman CL, Korsmeyer SJ, Cowburn D. Solution structure of the proapoptotic molecule BID: a structural basis for apoptotic agonists and antagonists. *Cell* 1999; **96**: 625–34.
24. Xu X-C. COX-2 inhibitors in cancer treatment and prevention, a recent development. *Anti-Cancer Drugs* 2002; **13**: 127–37.
25. Fukutake M, Nakatsugi S, Isoi T, *et al.* Suppressive effects of nimesulide, a selective inhibitor of cyclooxygenase-2, on azoxymethane-induced colon carinogenesis in mice. *Carcinogenesis* 1998; **19**: 1939–42.
26. Hida T, Kozaki K, Muramatsu H, *et al.* Cyclooxygenase-2 inhibitor induces apoptosis and enhances cytotoxicity of various anticancer agents in non-small cell lung cancer lines. *Clin Cancer Res* 2000; **6**: 2006–11.
27. Zhang Z, Dubois RN. Par-4, a proapoptotic gene, is regulated by NSAIDs in human colo carcinoma cells. *Gastroenterology* 2000; **118**: 1012–7.
28. Tardieu D, Jaeg JP, Deloly A, Corpet DE, Cadet J, Petit CR. The COX-2 inhibitor nimesulide suppresses superoxide and 8-hydroxy-deoxyguanosine formation, and stimulates apoptosis in mucosa during early colonic inflammation in rats. *Carcinogenesis* 2000; **21**: 973–6.
29. Nakatsugi S, Fukutake M, Takahashi M, *et al.* Suppression of intestinal polyp development by Nimesulide, a selective cyclooxygenase-2 inhibitor, in min mice. *Jpn J Cancer Res* 1997; **88**: 1117–20.
30. Taniguchi Y, Ikesue A, Yokoyama K, *et al.* Selective inhibition by nimesulide, a novel non-steroidal anti-inflammatory drug, with prostaglandin endoperoxide synthase-2 activity *in-vitro*. *Pharm Sci* 1995; **1**: 173–5.
31. Hsu AL, Ching TT, Wang DS, Song X, Rangnekar VM, Chen CS. The cyclooxygenase-2 inhibitor celecoxib induces apoptosis by blocking Akt activation in human prostate cancer cells independently of Bcl-2. *J Biol Chem* 2000; **275**: 11397–403.
32. Tsuji M, DuBois RN. Alterations in cellular adhesion and apoptosis in epithelial cells overexpressing prostaglandin endoperoxide synthase 2. *Cell* 1995; **83**: 493–501.
33. Ding HF, Lin YL, McGill G, *et al.* Essential role for caspase-8 in transcription-independent apoptosis triggered by p53. *J Biol Chem* 2000; **275**: 38905–11.
34. Liu XH, Kirschenbaum A, Yao S, Lee R, Holland JF, Levine AC. Inhibition of cyclooxygenase-2 suppresses angiogenesis and the growth of prostate cancer. *in vivo*. *J Urol* 2000; **164**: 820–5.
35. Liu CH, Chang SH, Narko K, *et al.* Overexpression of cyclooxygenase-2 is sufficient to induce tumorigenesis in transgenic mice. *J Biol Chem* 2001; **276**: 18563–9.
36. Zimmermann KC, Waterhouse NJ, Goldstein JC, Schuler M, Green DR. Aspirin induces apoptosis through release of cytochrome *c* from mitochondria. *Neoplasia* 2000; **2**: 505–13.
37. Chan TA, Morin PJ, Vogelstein B, Kinzler KW. Mechanisms underlying nonsteroidal anti-inflammatory drug-mediated apoptosis. *Proc Natl Acad Sci USA* 1998; **95**: 681–6.
38. Sheng H, Shao J, Morrow JD, Beauchamp RD, DuBois RN. Modulation of apoptosis and Bcl-2 expression by prostaglandin E_2 in human colon cancer cells. *Cancer Res* 1998; **58**: 363–6.
39. Liu XH, Yao S, Kirschenbaum A, Levine AC. NS398, a selective cyclooxygenase-2 inhibitor, induces apoptosis and down-regulates bcl-2 expression in LNCaP cells. *Cancer Res* 1998; **58**: 4245–9.
40. Baek SJ, Kim KS, Nixon JB, Wilson LC, Eling TE. Cyclooxygenase inhibitors regulate the expression of TGF-β superfamily member that has proapoptotic and antitumorigenic activities. *Mol Pharmacol* 2001; **59**: 901–8.
41. Zimowska W, Motyl T, Skierski J, *et al.* Apoptosis and Bcl-2 protein changes in L1210 leukaemic cells exposed to oxidative stress. *Apoptosis* 1997; **2**: 529–39.
42. Zimowska W, Motyl T, Waręski P, Skierski J, Płoszaj T, Orzechowski A. Apoptosis induced by serum deprivation and apoptogenic factors of cellular origin is dependent on *bcl-2* and *bax* expression in L1210 leukaemic cells. *Polish J Vet Sci* 2000; **3**: 63–71.
43. Kudla G, Montessuit S, Eskes R, *et al.* The destabilization of lipid membranes induced by the C-terminal fragment of caspase-8-cleaved Bid is inhibited by the N-terminal fragment. *J Biol Chem* 2000; **275**: 22713–8.
44. Polster BM, Kinnaly KW, Fiskum G. BH3 death domain peptide induces cell-type selective mitochondrial outer membrane permeability. *J Biol Chem* 2001; **276**: 37887–94.
45. Kim TH, Zhao Y, Barber MJ, Kuharsky DK, Yin XM. Bid-induced cytochrome *c* release is mediated by a pathway independent of mitochondrial permeability transition pore and Bax. *J Biol Chem* 2000; **275**: 39474–81.

(Received 10 April 2002; revised form accepted 9 July 2002)